

TECHNICAL REPORT ARBRL-TR-02231

COMPARISON OF PENETRATION CODES FOR
STRAIN MEASUREMENTS IN KINETIC
ENERGY PENETRATORS

TECHNICAL
LIBRARY

J. J. Misey
A. D. Gupta
J. D. Wortman

March 1980



US ARMY ARMAMENT RESEARCH AND DEVELOPMENT COMMAND
BALLISTIC RESEARCH LABORATORY
ABERDEEN PROVING GROUND, MARYLAND

Destroy this report when it is no longer needed.
Do not return it to the originator.

Secondary distribution of this report by originating
or sponsoring activity is prohibited.

Additional copies of this report may be obtained
from the National Technical Information Service,
U.S. Department of Commerce, Springfield, Virginia
22151.

The findings in this report are not to be construed as
an official Department of the Army position, unless
so designated by other authorized documents.

*The use of trade names or manufacturers' names in this report
does not constitute indorsement of any commercial product.*

REPORT DOCUMENTATION PAGE		READ INSTRUCTIONS BEFORE COMPLETING FORM
1. REPORT NUMBER TECHNICAL REPORT ARBRL-TR-02231	2. GOVT ACCESSION NO.	3. RECIPIENT'S CATALOG NUMBER
4. TITLE (and Subtitle) COMPARISON OF PENETRATION CODES FOR STRAIN MEASUREMENTS IN KINETIC ENERGY PENETRATORS		5. TYPE OF REPORT & PERIOD COVERED Final
		6. PERFORMING ORG. REPORT NUMBER
7. AUTHOR(s) J. J. MISEY A. D. GUPTA J. D. WORTMAN		8. CONTRACT OR GRANT NUMBER(s)
9. PERFORMING ORGANIZATION NAME AND ADDRESS US Army Ballistic Research Laboratory ATTN: DRDAR-BLT Aberdeen Proving Ground, MD 21005		10. PROGRAM ELEMENT, PROJECT, TASK AREA & WORK UNIT NUMBERS 1L162618AH80
11. CONTROLLING OFFICE NAME AND ADDRESS US Army Armament Research and Development Command US Army Ballistic Research Laboratory ATTN: DRDAR BL Aberdeen Proving Ground, MD 21005		12. REPORT DATE MARCH 1980
		13. NUMBER OF PAGES 27
14. MONITORING AGENCY NAME & ADDRESS (if different from Controlling Office)		15. SECURITY CLASS. (of this report) UNCLASSIFIED
		15a. DECLASSIFICATION/DOWNGRADING SCHEDULE
16. DISTRIBUTION STATEMENT (of this Report) Approved for public release; distribution unlimited.		
17. DISTRIBUTION STATEMENT (of the abstract entered in Block 20, if different from Report)		
18. SUPPLEMENTARY NOTES		
19. KEY WORDS (Continue on reverse side if necessary and identify by block number) Kinetic energy penetration Strain Measurements Forward Ballistic Technique HELP Code EPIC-2 Code		
20. ABSTRACT (Continue on reverse side if necessary and identify by block number) A two-dimensional finite-difference Eulerian hydrocode (HELP) and a two-dimensional finite-element Lagrangian code (EPIC-2) were used to measure response characteristics of a long steel rod with a hemispherical nose impacting a rolled homogeneous armor target at 0° obliquity and at an ordnance velocity. Surface strains were computed at three positions along the steel rod and these results were compared with published experimental data wherein the measuring devices were strain gages mounted on a long rod at prescribed locations in a forward ballistic testing set up. <div style="text-align: right;">(cont'd)</div>		

UNCLASSIFIED

SECURITY CLASSIFICATION OF THIS PAGE(When Data Entered)

Computational results from both codes have shown excellent agreement with the experimental data during the elastic phase of the deformation. However with the onset of plastic deformation agreement was dependent on the failure criteria incorporated in the codes. With the inclusion of failure models in the codes very good agreement was obtained in the eroding finite element model while the finite-difference code agreement deteriorated significantly at later times.

UNCLASSIFIED

SECURITY CLASSIFICATION OF THIS PAGE(When Data Entered)

TABLE OF CONTENTS

	Page
LIST OF ILLUSTRATIONS	5
I. INTRODUCTION	7
II. NUMERICAL METHODS	7
III. NORMAL IMPACT SIMULATION	9
IV. MATERIAL PROPERTIES	9
V. RESULTS	14
VI. CONCLUSIONS.	18
DISTRIBUTION LIST	22

LIST OF ILLUSTRATIONS

Figure		Page
1	Experimental Arrangement of Forward Ballistic Technique for Strain Measurements	10
2	EPIC-2 Computational Mesh for Strain-Time Measurements. .	11
3	Dynamic and Quasi-Static Relationships between Stress and Strain for S7 steel (UNIVAR)	13
4	Compressive Strain-Time Record at 20mm Gage Position (0-10 μ s)	15
5	Compressive Strain-Time Record at 20mm Gage Position (0-20 μ s)	16
6	Surface Velocity vs. Time at 20mm Gage Position	17
7	EPIC-2 Deformation Pattern at 15 Microseconds	19
8	HELP Deformation Pattern at 20 Microseconds	20

I. INTRODUCTION

Within the past two decades the response of materials to high velocity impact has been examined by experimental techniques employing foil resistance gages for strain measurements. Early work by Bluhm,¹ Arajs², and Lascher, Henderson, and Maynard³ employed a reverse ballistic technique wherein plates were impacted against stationary projectiles instrumented with strain gages of various types. However, this technique limited tests to low density targets and to low impact velocities. Recently G. E. Hauver⁴ developed a forward ballistic technique wherein a long rod, instrumented with several stages of strain gages, was impacted against a stationary target at velocities greater than 1000 meters per second. The measurements from tests employing the forward ballistic technique were ultimately intended to serve as a comparison with predictions from a computer code, to provide input data of material parameters for more exact computations, and to improve the simulation of the penetration process.

This paper complements the work of Mr. Hauver by taking one of his test conditions and performing a numerical simulation of the instrumented long rod impacting a hard target at an ordnance velocity.

II. NUMERICAL METHODS

The first method employed a finite element formulation in the two-dimensional Lagrangian code, EPIC-2, developed by Dr. Gordon Johnson⁵ of Honeywell. The second method used a finite difference scheme in the two-dimensional Eulerian code, HELP, developed by L. J. Hageman et al.⁶, at Systems, Science and Software.

¹ Bluhm, J. I., "Stresses in Projectiles During Penetration", Proc. Soc. Exptl. Stress Anal., Vol 13, pp. 167-181, 1956.

² Arajs, V., "An Investigation of Forces on a Projectile During Perforation of Thin Aluminum Plates", Masters Thesis, Air Force Inst. Tech., 1971

³ Lascher, F. R., Henderson, D., and Maynard, D., "Determination of Penetration Forcing Function Data for Impact Fuzes - Phase II", Technical Report AVSD-0306-75-RR, AVCO Systems Division, Wilmington, MA, 1975

⁴ Hauver, G. E., "Penetration with Instrumented Rods", Proc. 14th Meet. Soc. Eng. Science, pp. 106-109, November 1977.

⁵ Johnson, G. R., "Analysis of Elastic-Plastic Impact Involving Severe Distortions", Journal of Applied Mechanics, Vol 98, No. 3, September 1976

⁶ Hageman, L. J., Wilkins, D. E., Sedgewick, R. T. and Waddell, J. L., "HELP: A Multi-material Eulerian Program for Compressible Fluid and Elastic-Plastic Flows in Two Space Dimensions and Time", Systems, Science and Software, SSS-R-75-2654, July 1975.

The EPIC-2 code performs Elastic-Plastic Impact Computations in two dimensions for axisymmetric and plain strain problems. It also is capable of handling axisymmetric problems with spin. It is based on a Lagrangian finite element, lumped mass formulation. The equations of motion are integrated directly, rather than through the traditional stiffness matrix approach. Nonlinear material strength and compressibility effects are included to account for elastic-plastic flow and wave propagation. The code has material descriptions which include strain hardening, strain rate effects, thermal softening and failure. Mesh generators are included to produce quickly configurations such as flat plates, spheres, and rods with blunt, ogival, or conical nose shapes. Complex shapes can also be represented simply by providing an adequate assemblage of elements to represent the desired geometry. The elements are triangular in shape and are well suited to represent severe distortions generally occurring during high velocity impact.

Material failure is currently dependent on the equivalent plastic strain and the volumetric strain. The equivalent plastic strain, $\bar{\epsilon}_p$, is obtained by integrating the equivalent strain rate, $\dot{\bar{\epsilon}}_p$ with respect to time during plastic flow such that

$$\bar{\epsilon}_p(t + \Delta t) = \bar{\epsilon}_p(t) + \dot{\bar{\epsilon}}_p(t) \Delta t$$

where Δt is the integration time increment. The volumetric strain ϵ_V is obtained by observing the current and initial volume of the element in the following manner

$$\epsilon_V = V/V_0 - 1$$

When the failure criterion has been met for these two strains the equivalent tensile stress is set to zero, and no tensile or shear stress is allowed to develop in the failed element. The net result is that the failed element acts like a liquid inasmuch as it can develop hydrostatic compression with no shear or tensile stress. Another option is available wherein the element fails totally and all stresses and pressures are set equal to zero.

The HELP code is a multimaterial Eulerian computer program dealing with compressible fluids and elastic-plastic flows in two space dimensions and time. Although the code is basically Eulerian, free surfaces and material interfaces are located in a Lagrangian fashion throughout the computational grid. No material diffusion is permitted across these discrete interfaces.

The material model employed in HELP consists of an equation of state, a deviatoric constitutive relationship, a yield criterion and a failure criterion for each of the material packages employed in the calculation.

Material failure in HELP is governed by the failure criterion. A material is said to have failed when the material tension falls below a critical value indicated by $(\rho/\rho_0)_{\text{Min}}$. When this occurs

all the deviatoric stresses in the cell are zeroed out.

III. NORMAL IMPACT SIMULATION

The projectile-target configuration selected for the simulation is similar to that used by Mr. Hauver⁷ in the experimental phase. A schematic drawing of the experimental setup is shown in Figure 1. The projectile, an S7 steel rod, 254mm long, 8.1mm in diameter, with a hemispherical nose impacts the target at 0° obliquity at a striking velocity of 1000 m/s. The target is rolled homogenous armor, 101.6mm in diameter and 25.4mm thick. Type EP high elongation foil gages, manufactured by Micro-Measurements, Inc, were located at 20mm, 40mm, and 60mm distances from the nose of the projectile.

In the EPIC-2 code the rod portion of the projectile is configured on an axisymmetric mesh, shown in Figure 2, consisting of six columns of triangular elements while the nose is segmented into six hemispheric layers of elements. 749 nodes and 1272 elements are required to model the projectile. The target is configured to have uniform elements about the impact point and increasing in size in both radial and axial directions so that 1050 nodes and 1972 elements are needed to model the target. The strain calculations were made by computing the change in length of the surface element at the desired gage location.

In the HELP code the computational mesh contained 86 cells in the axial direction and 32 cells in the radial direction, however, the rod was represented by 8 rows of cells in the radial direction. At the region of impact the cells had an aspect ratio of 1 and increased in both directions in order to encompass the entire projectile-target configuration. The strain computations at the desired locations were computed by observing the change in adjoining massless passive Lagrangian tracer particles located just within the cylindrical surface.

IV. MATERIAL PROPERTIES

The material properties for the computations were obtained from the Solid Mechanics Branch of the Laboratory. These properties are shown in Table 1.

⁷Hauver, G. E., "Penetration with Instrumented Rods", International J. of Engng. Sci., Vol 16, pp. 871-877, 1978.

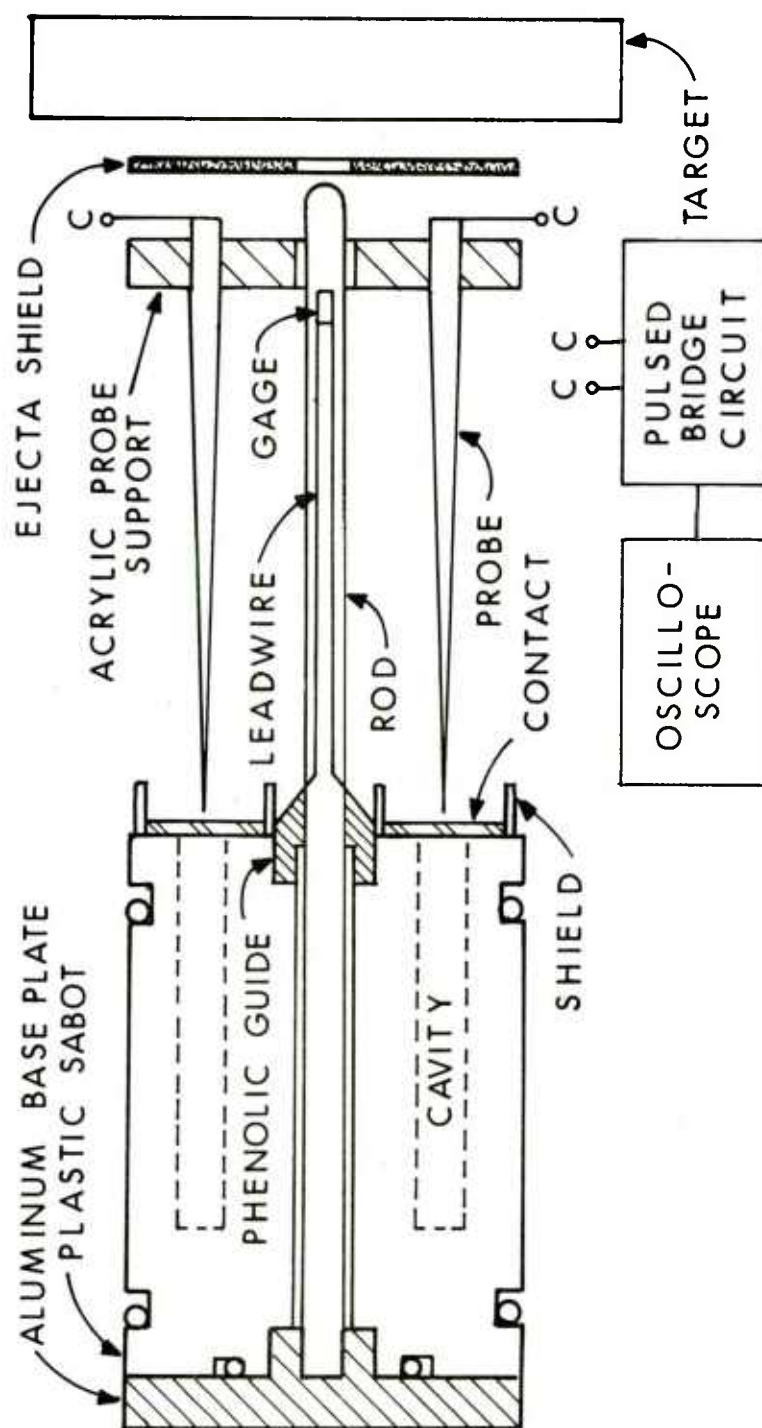


Figure 1. Experimental Arrangement of Forward Ballistic Technique for Strain Measurements

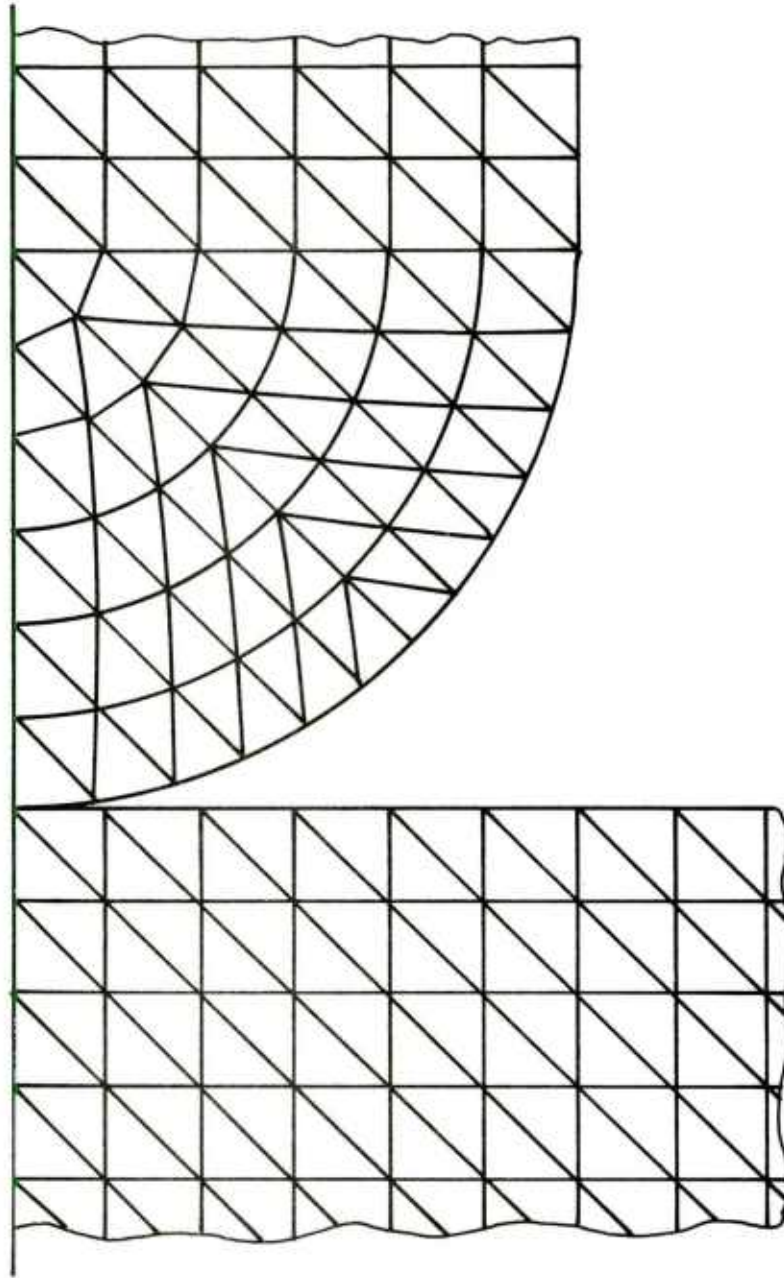


Figure 2. EPIC-2 Computational Mesh for Strain-Time Measurements

Table I. Material Properties

Material	ϵ	ν	σ_y	σ_u	ρ
	(GPa)		(GPa)	(GPa)	(Mg/m ³)
S7 steel	206.8	0.3	1.44	2.68	7.8
RHA	206.8	0.3	0.96	1.14	7.8

ϵ - elastic modulus

σ_u - ultimate strength

ν - Poisson's ratio

ρ - density

σ_y - yield strength

Dynamic and quasi-static tests were run to determine the elastic modulus and yield strength⁷. The results for S7 steel are shown in Figure 3. The ultimate strength was taken from data derived by Bell⁸.

In EPIC-2 the failure criterion was considered for two cases. In the first case failure was not allowed to occur in the projectile or target. For the second case only failure in the projectile was permitted in shear at a true strain of 40% and total failure at a true strain of 100%. These values for strain to failure were extrapolated from data for S7 steel obtained from Oak Ridge by Dr. E. W. Bloore⁹. The data indicated elongation at failure of 9.4 to 10.5% at a strain rate of 0.033 m/m/s and 20 to 22% at a strain rate of 280.0 m/m/s.

The failure criterion in the HELP code was based upon a minimum allowable density ratio defined as:

$$(\rho / \rho_o)_{\text{Min}} = -\frac{S}{K} + 1,$$

where K is the bulk modulus and S is the material spallation threshold. The values of the minimum density ratio for S7 steel and RHA were .972 and .986 respectively.

⁸Bell, J. F., "Theoretical and Experimental Studies of Shock Waves in Solids", Progress Report, Contract DAAD05-76-C-0722, BRL, APG, MD, May 1977

⁹Bloore, E. W., private communication.

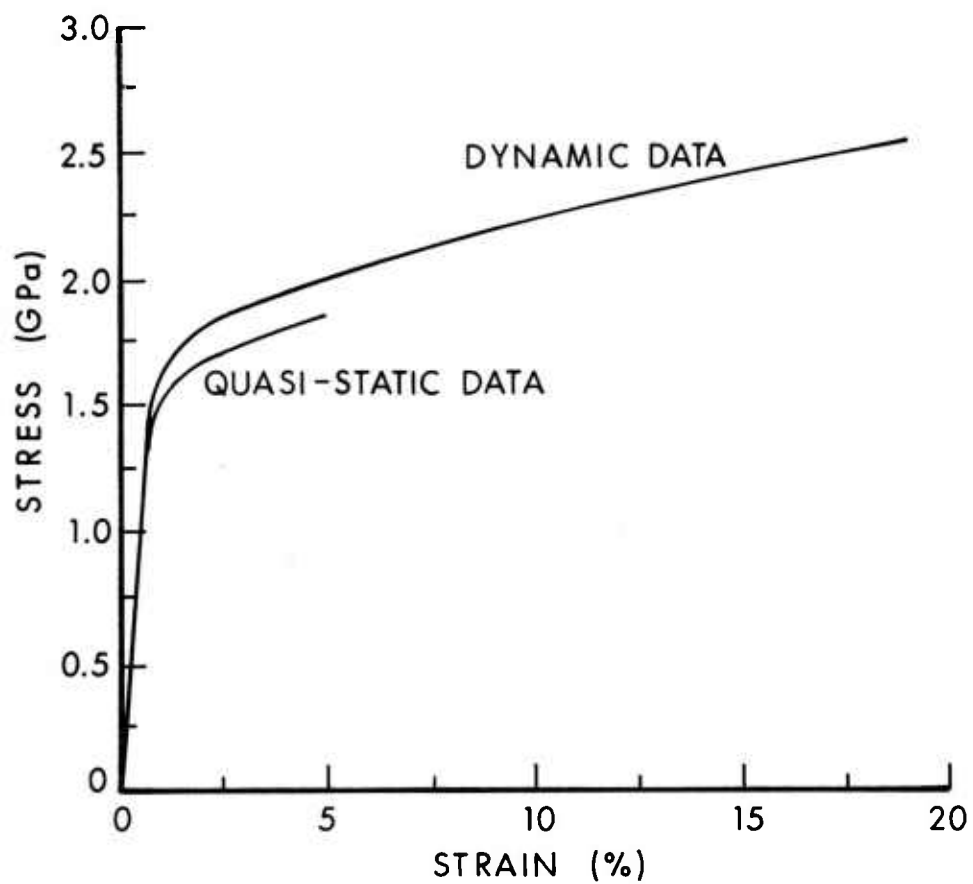


Figure 3. Dynamic and Quasi-Static Relations between Stress and Strain for S-7 Steel (UNIVAR)

V. RESULTS

The results from the computations and their comparison with the experimental values for surface strains at the 20mm position are shown in Figures 4 and 5. Figure 4 provides details of the elastic response portion of the strain-time record. Although there appears to be good agreement, the HELP calculation is greater and the EPIC calculations are less than the experimental value. However, at 8 microseconds, plastic deformation sets in and becomes the dominant feature. The strain in the EPIC-2 without failure calculation rises to a very high value while the other calculations remain at relatively low strains. The deviation becomes very dramatic, increasing rapidly to 47% strain by 20 microseconds. On the other hand the computations with penetrator failure in both HELP and EPIC-2 show good agreement until 18 microseconds. At this time the HELP code encounters difficulty in handling mixed cells and the strain deviates sharply, similar to the calculations without failure. Similar results occur at the 40 and 60mm gage positions.

The oscillation in the elastic portion of the strain-time record is due to reverberation of the tensile wave within the rod. This is demonstrated in Figure 6 which shows the computed radial velocity from EPIC-2 of a point on the surface of the projectile at the 20mm position as a function of time. On impact, two compressive stress waves are propagated. One moves up the rod, the other into the target. But at the same time, the intense stress in the rod is mitigated by tensile relief waves emanating from the lateral free surfaces of the rod. The rarefaction waves cross at the rod centerline and induce large tensile fields there. Such behavior has been previously noted by Wilkins and Guinan¹⁰ and by Mescall and Papirno¹¹ who have plotted elegant and illustrative contours of tensile stress in rods at very early times after impact. After several wave reverberations, the state of stress in the rod becomes quite complex and does not lend itself to simple representation. But this figure clearly shows the presence of tensile waves. The state of stress in the rod is two-dimensional and the smooth waveforms predicted by one-dimensional wave propagation theories should not be expected. It is worth noting that for very high-strength materials, such tensile waves can initiate fracture at the rod centerline; a phenomenon not explained by one-dimensional theories. Clearly, there is a tradeoff between high strength and ductility in long rod penetrator design.

¹⁰Wilkins, M. L., and Guinan, M. W., "Impact of Cylinders on a Rigid Boundary", *Journal of Applied Physics*, Vol 44, No. 3, pp. 1200-1206, March 1973.

¹¹Mescall, J., and Papirno, R., "Spallation in Cylinder-Plate Impact", *Experimental Mechanics*, Vol 14, No. 7, July 1974.

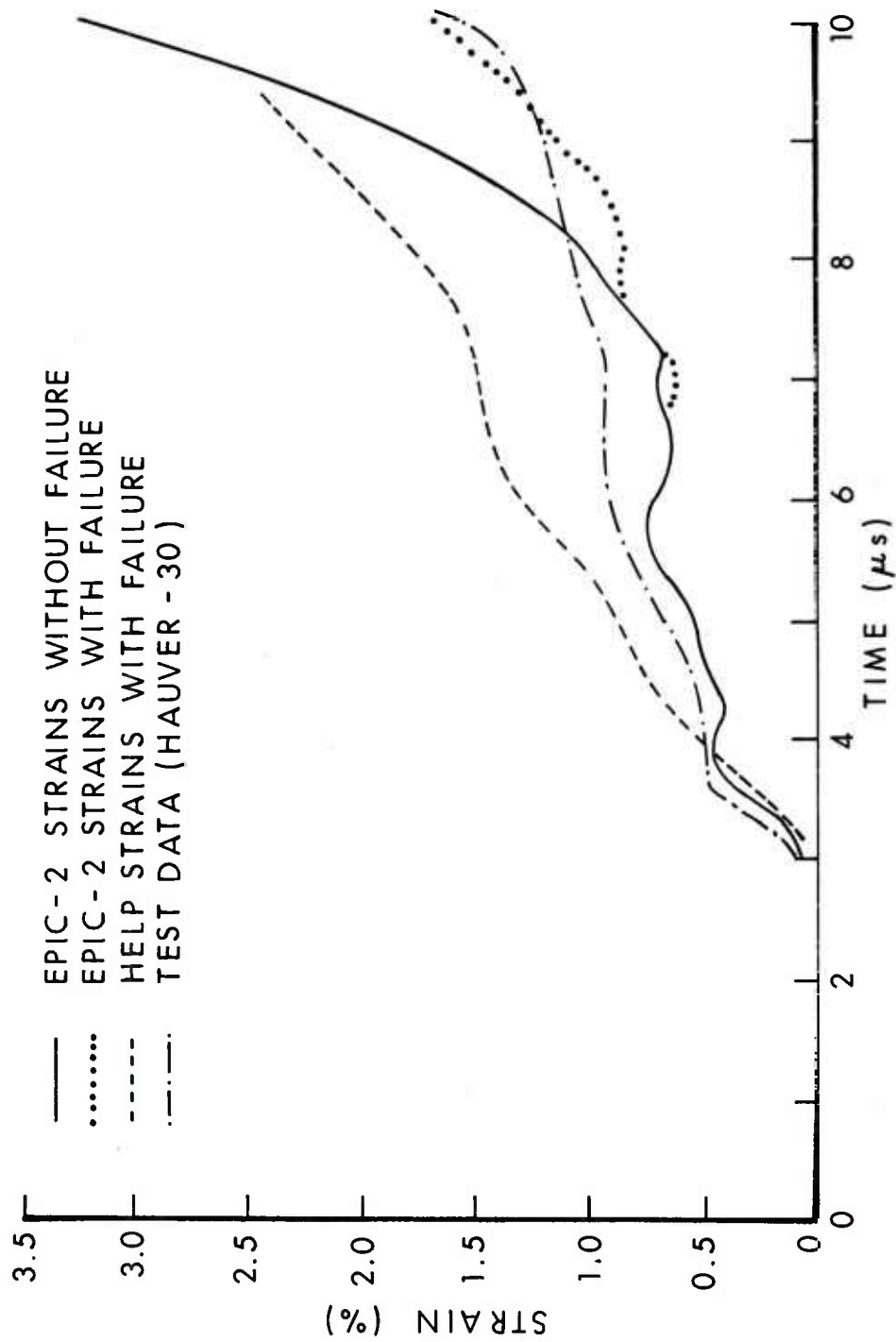


Figure 4. Compressive Strain-Time Record at 20mm Gage Position (0-10 μs)

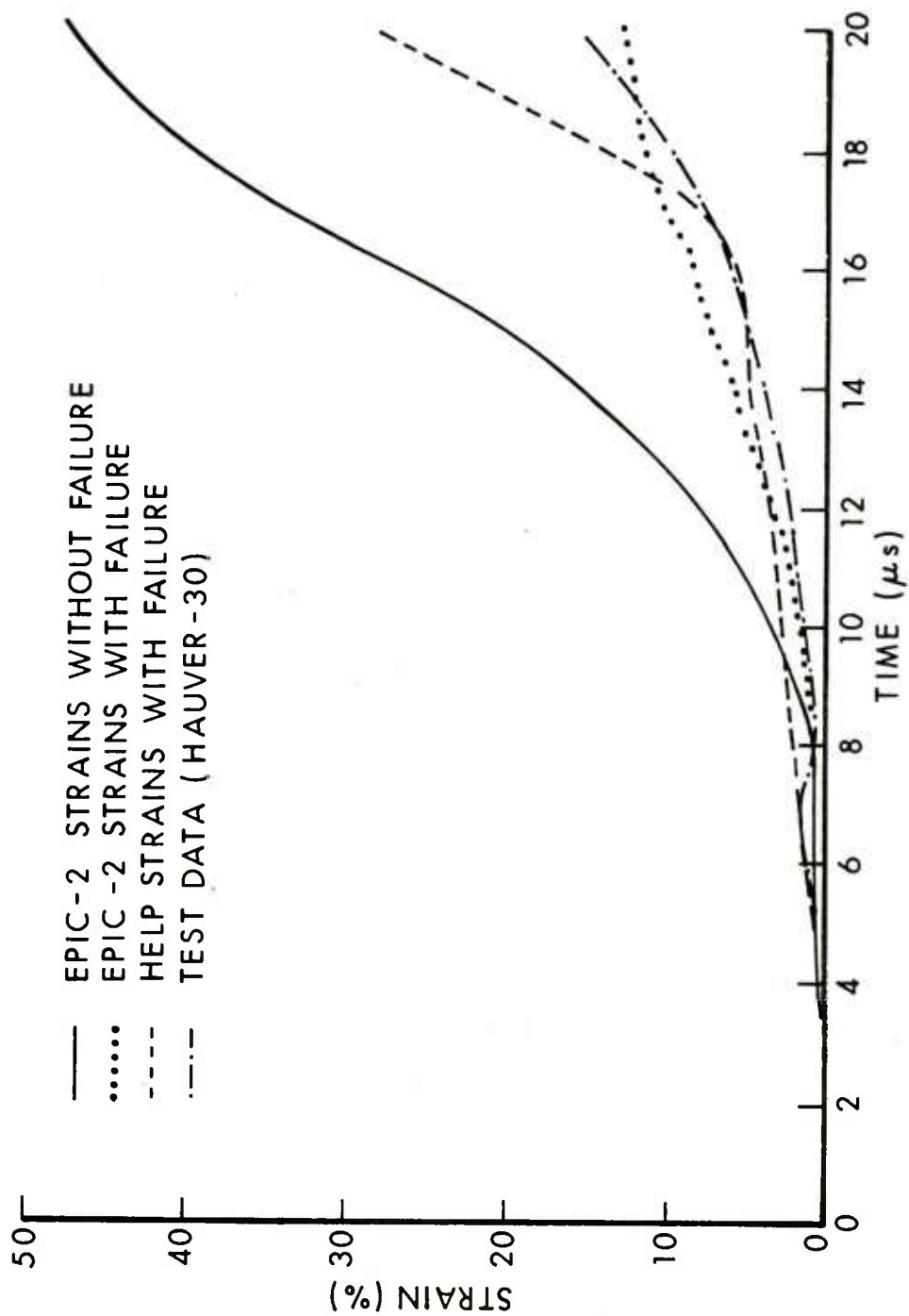


Figure 5. Compressive Strain-Time Record at 20mm Gage Position (0-20 μs)

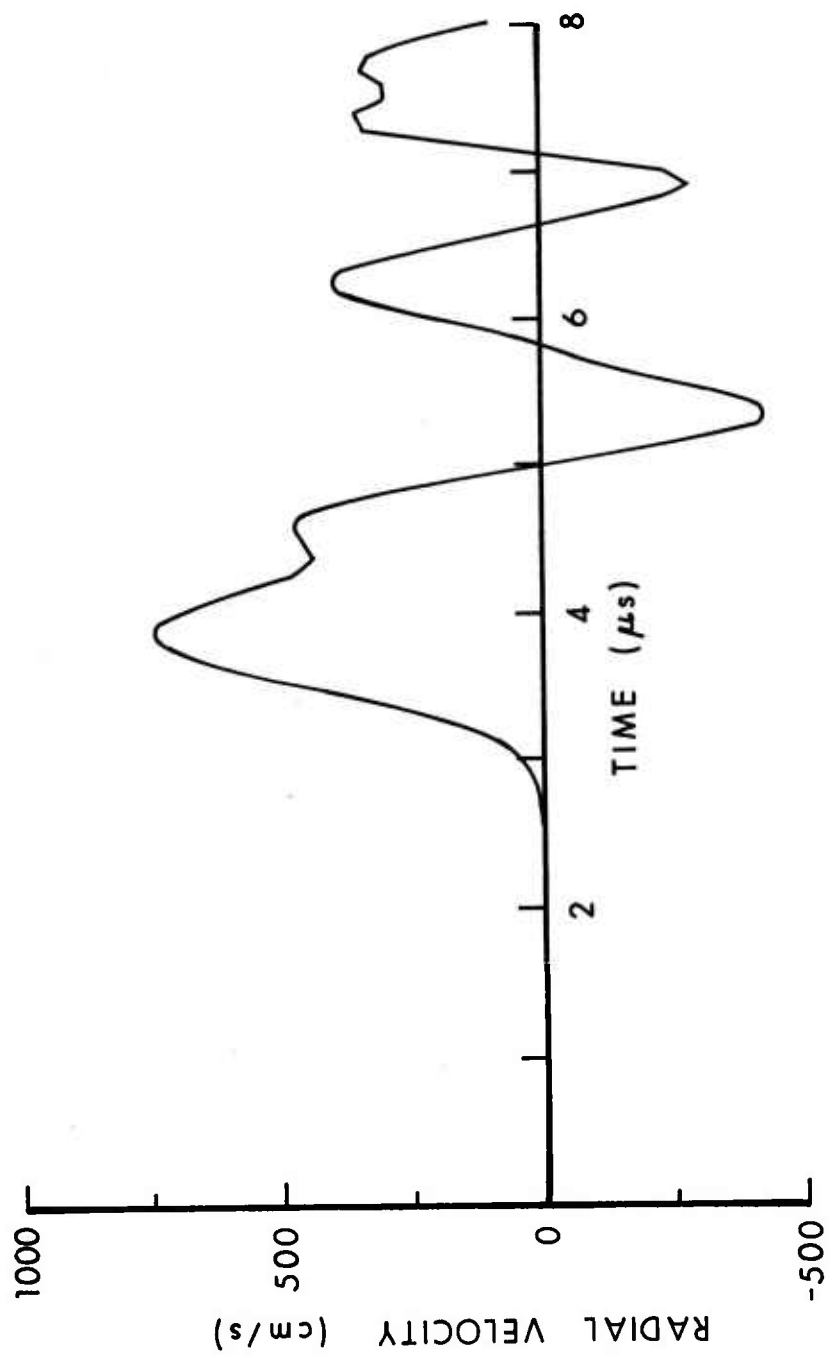


Figure 6. Surface Velocity vs Time at 20mm Gage Position

Typical deformation profiles for both EPIC-2 computations are shown in Figure 7. For the case with no failure all the elements are shown in the plot, and the usual erosion pattern is observed. However, for the case where projectile failure is allowed the elements, for which the tensile strain exceeds 100%, are ignored and are not shown in the plot. Hence the deformation profile shows only those elements still capable of carrying the load. The masses associated with the failed elements are nonetheless maintained in the computation.

EPIC-2 computations were also performed for four cases of failure condition. When only the target was allowed to fail the computed surface strains differed little from those where neither the target nor the projectile were allowed to fail. When both rod and target were allowed to fail the computed strains agreed closely with the case wherein only failure in the penetrator was permitted. Surface strains therefore are very much functions of penetrator deformation and failure modes and are little affected by details of target failure for this particular impact condition.

A typical deformation profile for the HELP computation is shown in Figure 8. Here the profile includes the failed elements and therefore introduces greater strain values than expected. It also shows significant acceleration of both materials at the projectile - target interface in a radial direction forming "ejecta" material at the interface. The absence of a smooth flow pattern is indicative of free surface tracer instability resulting in mixed cell problems and of the need for manually rezoning the projectile-target interface region.

VI. CONCLUSIONS

Numerical techniques exist for calculating the response of projectiles during the penetration and perforation of targets of finite thickness for impacts in the ordnance impact regime. The analysis of ballistic impact conditions and related phenomena can now be conducted through simulation techniques such as demonstrated by the EPIC-2 and the HELP codes.

It should be emphasized that computer codes such as those discussed here have advanced to the point where they can be used in conjunction with experimental procedures to advance the state-of-the-art in penetrator and armor design and effectiveness studies as well as armored systems vulnerability analyses. For the specific problems considered here the following conclusions can be drawn:

- a. Appropriate material failure models are essential for accurate prediction of penetrator response.

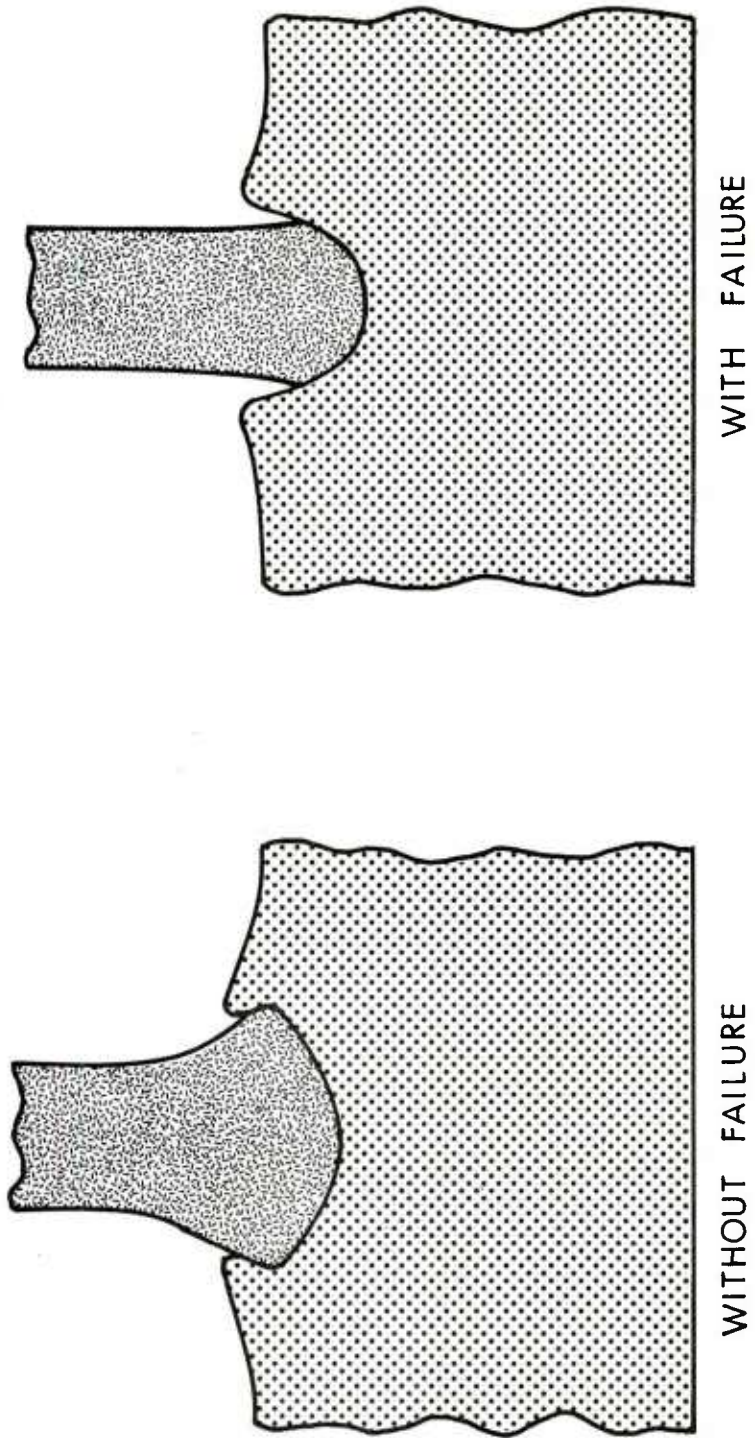


Figure 7. EPIC-2 Deformation Pattern at 15 Microseconds

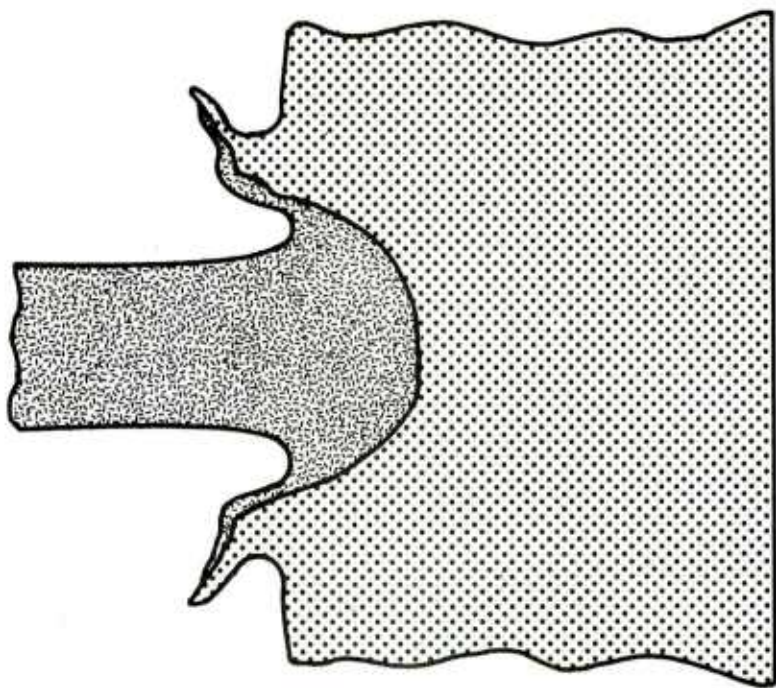


Figure 8. HELP Deformation Pattern at 20 Microseconds

b. Significant tensile stresses occur in the rod at early times after impact and are responsible for the oscillations in the elastic portion of both the experimental and computational strain-time records. It should be noted that for high strength materials with low ductility such tensile waves can cause failure along the penetrator centerline.

c. Surface strains in the penetrator are most strongly affected by failure of penetrator material at the rod-target interface and only marginally by failure of target material.

d. The Lagrangian method used in EPIC offers a better treatment for strain hardening and history dependent failure than is possible with Eulerian methods.

e. The Lagrangian calculation allows better resolution with less computer time; but because of the large amount of material distortion some elements at the interface can cause numerical instability which must be avoided by taking the affected cells out of the computational cycle.

f. The code predictions appear satisfactory during the initial elastic phase of the deformation but deteriorate significantly for the HELP code at longer time period due to severe plastic deformation of the nose and due to the limitations of plastic material modeling.

g. HELP code does not appear to be ideally suited for solving problems involving hemispherical-nosed projectiles with large length-to-diameter ratios and problems where the response is very sensitive to the failure properties of the penetrator material. However, the code may be useful for extremely high velocity impact problems where hydrostatic compression is significant.

Since very high plastic strains are encountered under ballistic impact conditions (up to 60% computed, 15% measured prior to gage failure), dynamic characterization of candidate materials for ballistic applications should be conducted at high strain rates (10^3 - 10^4 mm/mm/s) for very high strains. With the ready availability of two- and three-dimensional codes for studying penetration and perforation phenomena characterization under biaxial and triaxial loading conditions is imperative.

DISTRIBUTION LIST

<u>No. of</u> <u>Copies</u>	<u>Organization</u>	<u>No. of</u> <u>Copies</u>	<u>Organization</u>
12	Commander Defense Technical Info Center ATTN: DDC-DDA Cameron Station Alexandria, VA 22314	1	Commander US Army Materiel Development and Readiness Command ATTN: DRCDMD-ST 5001 Eisenhower Avenue Alexandria, VA 22333
1	Director Defense Advanced Research Projects Agency ATTN: Tech Info 1400 Wilson Boulevard Arlington, VA 22209	5	Commander US Army Armament Research and Development Command ATTN: DRDAR-TD, Dr. R. Weigle DRDAR-LC, Dr. J. Frasier DRDAR-SC, Dr. D. Gyorog DRDAR-LCF, G. Demitrack DRDAR-LCA, G. Randers-Pehrson Dover, NJ 07801
1	Director Defense Nuclear Agency Arlington, VA 22209	6	Commander US Army Armament Research and Development Command ATTN: DRDAR-SCS-M, R. Kwatnoski DRDAR-SCA-T, H. Kahn P. Ehle DRDAR-LCU, E. Barrieres DRDAR-TSS (2 cys) Dover, NJ 07801
1	Deputy Assistant Secretary of the Army (R&D) Department of the Army Washington, DC 20310	1	Commander US Army Armament Materiel Readiness Command ATTN: DRSAR-LEP-L, Tech Lib Rock Island, IL 61299
1	Commander US Army BMD Advanced Technology Center ATTN: BMDATC-M, Mr. P. Boyd PO Box 1500 Huntsville, AL 35807	1	Commander US Army Aviation Research and Development Command ATTN: DRSAR-E 12th and Spruce Streets St. Louis, MO 63166
1	HQDA (DAMA-ARP) WASH DC 20310		
1	HQDA (DAMA-MS) WASH DC 20310		
2	Commander US Army Engineer Waterways Experiment Station ATTN: Dr. P. Hadala Dr. B. Rohani PO Box 631 Vicksburg, MS 39180		

DISTRIBUTION LIST

<u>No. of</u> <u>Copies</u>	<u>Organization</u>	<u>No. of</u> <u>Copies</u>	<u>Organization</u>
1	Director US Army Air Mobility Research and Development Laboratory Ames Research Center Moffett Field, CA 94035	1	Commander TARADCOM Tank-Automotive Systems Laboratory ATTN: T. Dean Warren, MI 48090
1	Commander US Army Communications Research and Development Command ATTN: DRDCO-PPA-SA Fort Monmouth, NJ 07703	7	Director US Army Materials and Mechanics Research Center ATTN: DRXMR-T, Mr. J. Bluhm Mr. J. Mescall Dr. M. Lenoe R. Shea F. Mascianica E. Quigley DRXMR-ATL Watertown, MA 02172
1	Commander US Army Electronics Research and Development Command Technical Support Activity ATTN: DELSD-L Fort Monmouth, NJ 07703		
2	Commander US Army Missile Command ATTN: DRDMI-R DRDMI-RBL Redstone Arsenal, AL 35809	1	Commander US Army Research Office ATTN: Dr. E. Saibel Dr. G. Mayer PO Box 12211 Research Triangle Park NC 27709
1	Commander US Army Missile Command ATTN: DRDMI-YDL Redstone Arsenal, AL 35809	1	Director US Army TRADOC Systems Analysis Activity ATTN: ATAA-SL (Tech Lib) White Sands Missile Range NM 88002
1	Commander US Army Tank-Automotive Re- search and Development Command ATTN: DRDTA-UL Warren, MI 48090	1	Office of Naval Research Department of the Navy ATTN: Code ONR 439, N. Perrone 800 North Quincy Street Arlington, VA 22217
1	Commander US Army Tank-Automotive Re- search and Development Command ATTN: V. H. Pagano Warren, MI 48090	3	Commander Naval Air Systems Command ATTN: AIR-604 Washington, DC 20360

DISTRIBUTION LIST

<u>No. of Copies</u>	<u>Organization</u>	<u>No. of Copies</u>	<u>Organization</u>
3	Commander Naval Ordnance Systems Command Washington, DC 20360	3	Director Naval Research Laboratory ATTN: Dr. C. Sanday Dr. H. Pusey Dr. F. Rosenthal Washington, DC 20375
2	Commander Naval Air Development Center, Johnsville Warminster, PA 18974	2	Superintendent Naval Postgraduate School ATTN: Dir of Lib Dr. R. Ball Monterey, CA 93940
1	Commander Naval Missile Center Point Mugu, CA 93041	2	ADTC/DLJW (Ms. C. Westmoreland/ Mr. W. Cook) Eglin AFB, FL 32542
2	Naval Ship Engineering Center ATTN: J. Schell Tech Lib Washington, DC 20362	1	AFML/LLN (Dr. T. Nicholas) Wright-Patterson AFB, OH 45433
1	Commander & Director David W. Taylor Naval Ship Research & Development Center Bethesda, MD 20084	1	Lawrence Livermore Laboratory PO Box 808 ATTN: Dr. D. M. Norris Livermore, CA 94550
2	Commander Naval Surface Weapons Center ATTN: Dr. W. G. Soper Mr. N. Rupert Dahlgren, VA 22448	1	Lawrence Livermore Laboratory PO Box 808 ATTN: Dr. M. L. Wilkins Livermore, CA 94550
2	Commander Naval Surface Weapons Center Silver Spring, MD 20084	1	Lawrence Livermore Laboratory PO Box 808 ATTN: Dr. R. Werne Livermore, CA 94550
7	Commander Naval Weapons Center ATTN: Code 31804, Mr. M. Keith Code 326, Mr. P. Cordle Code 3261, Mr. T. Zulkoski Code 3181, John Morrow Code 3261, Mr. C. Johnson Code 3171, Mr. B. Galloway Code 3813, Mr. M. Backman China Lake, CA 93555	4	Los Alamos Scientific Laboratory PO Box 1663 ATTN: Dr. R. Karpp Dr. J. Dienes Dr. J. Taylor Dr. E. Fugelso Los Alamos, NM 87545

DISTRIBUTION LIST

<u>No. of Copies</u>	<u>Organization</u>	<u>No. of Copies</u>	<u>Organization</u>
3	Sandia Laboratories ATTN: Dr. W. Herrmann Dr. L. Bertholf Dr. A. Chabai Albuquerque, NM 87115	1	Computer Code Consultants 1680 Camino Redondo ATTN: Dr. Wally Johnson Los Alamos, NM 87544
1	Headquarters National Aeronautics and Space Administration Washington, DC 20546	1	Dupont Experimental Labs ATTN: Dr. Carl Zweben Wilmington, DE 19801
1	Director National Aeronautics and Space Administration Langley Research Center Langley Station Hampton, VA 23365	1	Effects Technology Inc 5383 Hollister Avenue PO Box 30400 Santa Barbara, CA 93105
1	Aeronautics Research Associates of Princeton, Inc 50 Washington Road Princeton, NJ 08540	2	Falcon R&D Thor Facility ATTN: Mr. D. Malick Mr. J. Wilson 696 Fairmount Avenue Baltimore, MD 21204
2	Aerospace Corporation 2350 E. El Segundo Blvd ATTN: Mr. L. Rubin Mr. L. G. King El Segundo, CA 90245	1	FMC Corporation Ordnance Engineering Div San Jose, CA 95114
2	Battelle Columbus Laboratories ATTN: Dr. M. F. Kanninen Dr. G. T. Hahn 505 King Avenue Columbus, OH 43201	1	General Electric Company Armament Systems Dept Burlington, VT 05401
1	Boeing Aerospace Company ATTN: Mr. R. G. Blaisdell (M.S. 40-25) Seattle, WA 98124	1	President General Research Corporation ATTN: Lib McLean, VA 22101
		1	Goodyear Aerospace Corp 1210 Massillon Rd Akron, OH 44315
		1	H. P. White Laboratory 3114 Scarboro Road Street, MD 21154

DISTRIBUTION LIST

<u>No. of</u> <u>Copies</u>	<u>Organization</u>	<u>No. of</u> <u>Copies</u>	<u>Organization</u>
3	Honeywell, Inc Government & Aerospace Products Division ATTN: Mr. J. Blackburn Dr. G. Johnson Mr. R. Simpson 600 Second Street, NE Hopkins, MN 55343	1	Science Applications Inc 101 Continental Blvd Suite 310 El Segundo, CA 90245
1	International Applied Physics, Inc 2400 Glenheath Drive ATTN: Mr. H. F. Swift Kettering, OH 45440	1	Ship Systems, Inc. 11750 Sorrento Valley Road ATTN: Dr. G. G. Erickson San Diego, CA 92121
1	Kaman Sciences Corp 1500 Garden of the Gods Road ATTN: Dr. P. Snow Colorado Springs, CO 80933	1	Systems, Science and Software, Inc PO Box 1620 ATTN: Dr. R. Sedgwick La Jolla, CA 92038
1	Lockheed Palo Alto Research Laboratory 3251 Hanover Street ATTN: Org. 5230, Bldg. 201 Mr. R. Roberson Palo Alto, CA 94394	1	US Steel Corp Research Center 125 Jamison Lane Monroeville, Pa 15146
1	Materials Research Laboratory Inc 1 Science Road Glenwood, IL 60427	1	Drexel University Department of Mechanical Engineering ATTN: Dr. P. C. Chou 32d and Chestnut Streets Philadelphia, PA 19104
2	McDonnell-Douglas Astronautics Co 5301 Bolsa Avenue ATTN: Dr. L. B. Greszczuk Dr. J. Wall Huntington Beach, CA 92647	1	New Mexico Institute of Mining and Technology ATTN: TERA Group Socorro, NM 87801
1	Pacific Technical Corp 460 Ward Drive ATTN: Dr. F. K. Feldmann Santa Barbara, CA 93105	1	Forrestall Research Center Aeronautical Engineering Laboratory Princeton University ATTN: Dr. A. Eringen Princeton, NJ 08540

DISTRIBUTION LIST

<u>No. of Copies</u>	<u>Organization</u>	<u>No. of Copies</u>	<u>Organization</u>
3	Southwest Research Institute Department of Mechanical Sciences ATTN: Dr. U. Lindholm Dr. W. Baker Dr. R. White 8500 Culebra Road San Antonio, TX 78228		<u>Aberdeen Proving Ground</u> Cdr, USATECOM ATTN: Mr. W. Pless Mr. S. Keithley DRSTE-TO-F Dir, USAMSAA ATTN: DRXSY-D DRXSY-MP, H. Cohen Dir, Wpns Sys Concepts Team Bldg. E3516, EA ATTN: DRDAR-ACW
3	SRI International 333 Ravenswood Avenue ATTN: Dr. L. Seaman Dr. L. Curran Dr. D. Shockey Menlo Park, CA 94025		
2	University of Arizona Civil Engineering Department ATTN: Dr. D. A. DaDeppo Dr. R. Richard Tucson, AZ 86721		
1	University of California Department of Physics ATTN: Dr. Harold Lewis Santa Barbara, CA 93106		
2	University of Delaware Department of Mechanical Engineering ATTN: Prof. J. Vinson Dean I. Greenfield Newark, DE 19711		
1	University of Denver Denver Research Institute ATTN: Mr. R. F. Recht 2390 South University Boulevard Denver, CO 80210		

USER EVALUATION OF REPORT

Please take a few minutes to answer the questions below; tear out this sheet and return it to Director, US Army Ballistic Research Laboratory, ARRADCOM, ATTN: DRDAR-TSB, Aberdeen Proving Ground, Maryland 21005. Your comments will provide us with information for improving future reports.

1. BRL Report Number _____

2. Does this report satisfy a need? (Comment on purpose, related project, or other area of interest for which report will be used.)

3. How, specifically, is the report being used? (Information source, design data or procedure, management procedure, source of ideas, etc.) _____

4. Has the information in this report led to any quantitative savings as far as man-hours/contract dollars saved, operating costs avoided, efficiencies achieved, etc.? If so, please elaborate.

5. General Comments (Indicate what you think should be changed to make this report and future reports of this type more responsive to your needs, more usable, improve readability, etc.) _____

6. If you would like to be contacted by the personnel who prepared this report to raise specific questions or discuss the topic, please fill in the following information.

Name: _____

Telephone Number: _____

Organization Address: _____
